Modeling and Simulation of the Polymeric Nanocapsule Formation Process

Luciane S. Ferreira and Jorge O. Trierweiler

GIMSCOP – Chemical Engineering Department – UFRGS. Rua Luis Englert, s/n. Porto Alegre. RS. Brasil.
(e-mail: {luciane,jorge}@enq.ufrgs.br)

Abstract: In this work the modelling and simulation of nanoparticle formation according to the technique of nanoprecipitation was done. In this method, the particle is formed due to the further diffusion of solvent into the water, resulting in the aggregation of the associated polymer chains. In order to predict the characteristics of the nanoparticle and also to improve the process, it was developed a mathematical model that considers: (a) the type of polymer; (b) interaction between solvent and polymer; and, (c) dynamics of solvent diffusion. The diffusivity between polymer-solvent was modelled by means of the Vrentas & Duda Free Volume Theory, including the Sanchez-Lacombe equation-of-state. The model was written in terms of Partial Differential Equation, and solved with MAPLE for a given initial size distribution. Additionally, it is a moving boundary problem because the diffusion of the solvent out of the droplet leads to its size reduction. Based on a given initial droplet size distribution, the transient behaviour and the final droplet size distribution can be evaluated. The dynamic simulation shows both the evolution of the solvent inside the droplet and the variation of size in time. Additionally, the comparison between experimental and simulated results showed a very good agreement.

Keywords: nanoprecipitation, modeling, simulation, diffusion, moving boundary, droplet size distribution.

1. INTRODUCTION

Polymeric nanoparticles are of especial interest from the pharmaceutical point of view. First, they are more stable in the gastrointestinal tract than other colloidal carriers and can protect encapsulated drugs from gastrointestinal environment. Second, the use of various polymeric materials enable the modulation of physicochemical characteristics (e.g. hydrophobicity, zeta potential), drug release properties, and biological behavior (e.g. targeting, bioadhesion, improved cellular uptake) of nanoparticles. Finally, their submicron size and large specific surface area favor their absorption compared to larger carriers (Des Rieux *et al.*, 2006). For instance, nanoparticles encapsulating proteins and vaccines (Des Rieux *et al.*, 2006) and chemotherapeutic agents (Jabr-Milane *et al.*, 2008) have been investigated in the last years.

One of the methods applied to produce nanoparticles is the so-called Nanoprecipitation. This method, first presented in 1989 (Fessi *et al.*, 1989), was largely applied by other authors in the subsequent years (Guterres *et al.*, 1995, Thioune *et al.*, 1997, Govender *et al.*, 1999, Chorny *et al.*, 2002, Galindo-Rodriguez *et al.*, 2004, Bilati *et al.*, 2005, Galindo-Rodriguez *et al.*, 2005). It consists of a simple procedure for the preparation of nanocapsules (NC) by interfacial deposition of a preformed, well-defined, and biodegradable polymer following displacement of a semi-polar solvent miscible with water from a lipophilic solution. The method of preparation yielded spherical vesicular nanocapsules, which consisted of an oily cavity – where the drug is dissolved - surrounded by a thin wall formed by interfacial deposition of the polymer. When organic and aqueous phases are in contact, it is assumed that solvent diffuses from the organic phase into the water and carries with it some polymer chains, which are still in solution. Then, as the solvent diffuses further into the water, the associated polymer chains aggregate forming NC. Therefore, this method involves the equilibrium among a polymer, its solvent and a non-solvent.

In order to predict the characteristics of the nanoparticle and also to improve the process, it was developed a mathematical model that takes in account: (a) the type of polymer; (b) interaction between solvent and polymer; and, (c) solvent diffusion process. After the description of the nanocapsules preparation, the mathematical model is explained. Then, the numerical simulation and its results are discussed. Finally, in the appendix the Free Volume model, applied to calculate the diffusivity polymer/solvent, is explained.

2. NANOCAPSULES PREPARATION

As mentioned in the previous section, the nanocapsules are prepared according to the method of nanoprecipitation. This method is based on the spontaneous emulsification of the organic internal phase, in which the polymer is dissolved, into the external aqueous phase. In this work nanocapsules of poly(ε-caprolactone) (PCL) containing 3-benzophenon (solar protection factor) were prepared according to the following procedure (Fessi *et al.*, 1989): 100 mg of PCL, 76.6 mg of sorbitan monostearate, 333 mg of Mygliol 810 (caprylic/capric triglyceride) and 30mg of Benzophenon-3 are first dissolved in acetone (27 ml). The resulting organic solution is poured in 53 ml of water containing 76.6 mg of polysorbate 80. The aqueous phase immediately turns milky with bluish opalescence as a result of the formation of nanocapsules, the wall of which is mainly constituted by PCL, and the oily core by the benzophenon-mygliol solution. The size of the nanoparticles is then analyzed by *Dynamic Light Scattering* (Zetasizer Nano, Malvern).

3. MATHEMATICAL MODELLING

It was considered that the nanoprecipitation produces perfect spherical particles and also that each nanoparticle is originated from one droplet formed immediately after the mixing of organic phase and aqueous phases. The major model assumptions are: (a) there is a negligible relative velocity between the droplet and the water; therefore, the external mass transfer is approximated by diffusion. This assumption can be done based on the order of the Stokes number, which is related to the particle velocity and is defined as (Crowe, 2005, Rielly and Marquis, 2001):

$$St \equiv \frac{\tau_v}{\tau_F} = \frac{d_p^{\,2}\rho_p V}{18\mu L} \quad [1] \tag{1}$$

For small Stokes numbers, the particles follow the fluid motion; but for large *St*, the particles follow different trajectories from the fluid elements. The Stokes number (Figure 1) was calculated for fluid velocities between $1x10^{-3}$ and 1 $m.s^{-1}$ (based on CFD simulations for a stirred tank that are not showed here), and particle diameters from 100 to 4000 nm. As the Stoke number is in all cases less than 10^{-5}, the assumption of negligible relative velocity between the droplets and the external phase can be considered valid.

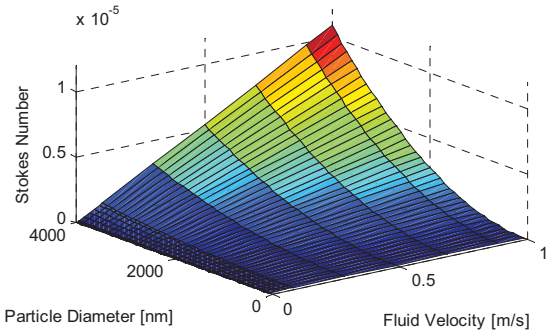

Fig. 1. Stokes Number.

(b) the diffusion is one-dimensional along the radial direction; and, (c) the diffusivity varies with time and concentration only.

Based on these assumptions, the mass balance equation for the solvent, written in spherical coordinates is:

$$\frac{\partial c_1(r,t)}{\partial t} = \frac{D}{r^2}\left(\frac{\partial}{\partial r}\left(r^2\left(\frac{\partial c_1(r,t)}{\partial r}\right)\right)\right) \quad [2] \tag{2}$$

This is a moving boundary problem, since the size of the droplet reduces because of the diffusion.

As the dimensions of dependent and independent variables are not the same, a variable normalization was be done including new variables τ, *rh*, and c_{1h} defined as,

$$t_0 = \frac{r_0^2}{D} \tag{3}$$

$$\left\{r = rh \cdot r_0,\ t = \tau \cdot t_0,\ c_1(r,t) = c_{1h}(rh,\tau)\cdot\rho_1\right\} \quad [3] \tag{4}$$

After the normalization, (2) is then rewritten as:

$$\frac{1}{t_0}\cdot\frac{\partial c_{1h}(rh,\tau)}{\partial \tau} = \frac{D}{r_0^{\,2}\cdot rh^2}\left(\frac{\partial}{\partial rh}\left(rh^2\left(\frac{\partial c_{1h}(rh,\tau)}{\partial rh}\right)\right)\right). \tag{5}$$

3.1 Initial and Boundary Conditions

It is assumed that the solution is well mixed and therefore, the concentration inside the droplet is uniform. Thus the initial condition is,

$$c_{1h}(rh,0) = c_{1h0} \qquad 0 \le rh \le r0\,. \tag{6}$$

Where c_{1h0} is evaluated according to the experimental conditions.

The boundary condition at the center of the droplet (rh=0) arises from the symmetry,

$$\left.\frac{dc_{1h}}{drh}\right|_{rh=0} = 0 \qquad t \ge 0\,. \tag{7}$$

Additionally, the boundary condition at the interface was calculated based on the mass balance and can be written as

$$\left.\frac{dc_{1h}}{dt}\right|_{rh=R} = \frac{D_{S-W}}{4\pi R^2}\left(c_{1h}(R) - c_{1h}(\infty)\right) \quad [4] \tag{8}$$

3.2 Boundary Movement

The boundary movement is calculated based on the assumption that both the mass of polymer, oil and drug remain constant during the diffusion process. The volume of the droplet is considered to be

$$V_D = V_2 + V_1 + V_{oil} + V_{drug} \equiv \frac{4}{3}\pi R^3 \quad [5] \tag{9}$$

Per definition the volume of polymer and solvent inside the droplet are

$$V_2 = m_2/\rho_2 \qquad V_1 = (c_1/\rho_1)V_D \quad [6] \tag{10}$$

Substituting (10) in (9) and isolating for *R*, then the radius can be calculated as

$$R(t) = \sqrt[3]{\left[3\cdot\left(\frac{m_2}{\rho_2} + V_{oil} + V_{drug}\right)\cdot\left(1 - \frac{c_1(t)}{\rho_1}\right)^{-1}\right] \Big/ 4\pi}\,. \tag{11}$$

3.3 Model Parameters

The two main parameters of this model are the diffusivity solvent/polymer and the diffusivity solvent/water.

The experimental data presented by Wild (2003) was adjusted as a polynomial curve to describe the diffusivity of acetone in water.

$$D_{S\text{-}W} = -4.737 w_S + 15.92\ w_S - 14.71\ w_S + 4.738 \tag{12}$$

where w_s is the molar fraction of water in the external phase.

The diffusivity between polymer and solvent was modelled according to the Free Volume Theory (Vrentas and Duda, 1976, Vrentas and Duda, 1977a, Vrentas and Duda, 1977b, Vrentas and Duda, 1979). Those authors applied the Flory–Huggins thermodynamic model in their free volume diffusion theory to describe the polymer solvent enthalpic and entropic

---

[1] τ_F - characteristic time of the flow field; τ_v - particle relaxation time; d_p - particle diameter; ρ_p - particle density; *V* - fluid velocity, μ - fluid viscosity; *L* - characteristic dimension of the obstacle.

[2] c_1 - concentration of solvent; *r* - particle radius; *D* - diffusivity; *t* - time.

[3] r_0 - initial droplet radius; *D* - diffusivity; ρ_1 - solvent density.

[4] *R* - actual radius of the droplet; $D_{S\text{-}W}$ - diffusivity of the solvent in the external phase; $c_{1h}(R)$ - concentration of solvent at the interface; $c_{1h}(\infty)$ - bulk concentration.

[5] V_D - volume of the droplet; V_1, V_2, V_{oil}, V_{drug} - volume of solvent, polymer, oil, and drug, respectively.

[6] m_2 - mass of polymer; ρ_2 - polymer density.

interactions. For the estimation of solvent diffusion coefficient in polymer solution systems, free-volume parameters for the both polymer and solvent must be available. The free volume (FV) diffusion model developed by Vrentas & Duda describes the solvent self-diffusion coefficient (D_1) and the polymer/solvent binary mutual diffusion coefficient (D) as given by (13) and (14), respectively.

$$D_1 = D_0 \exp\left(\frac{-E}{RT}\right)\cdot\exp\left(\frac{-\left(w_1\hat{V}_1^* + w_2\xi\hat{V}_2^*\right)}{w_1\left(\frac{K_{11}}{\gamma}\right)\left(K_{21}-T_{g1}+T\right)+w_2\left(\frac{K_{12}}{\gamma}\right)\left(K_{22}-T_{g2}+T\right)}\right) \quad (13)$$

$$D = D_1\left(1-\phi_1\right)^2\left(1-2\chi\phi_1\right) \quad (14)$$

In (13) the first exponential term can be considered as the energy factor, and the second exponential term is the free-volume factor. Eq. (14) contains the following implicit assumptions (Zielinski and Duda, 1992): (a) the mutual-diffusion coefficient is related theoretically to the solvent and polymer self-diffusion coefficients through an expression developed by Bearman (1961); (b) the contribution of the polymer self-diffusion coefficient to the mutual-diffusion is negligible; and, (c) the Flory-Huggins (Flory, 1970) model accurately describes the polymer activity. In addition, the specific free volumes of the polymer and solvent are presumed to be additive (without a volume change on mixing), and thermal expansion coefficients are approximated by average values over the temperature intervals of interest (Frick *et al.*, 1990, Lodge *et al.*, 1990). There are 13 independent parameters to be evaluated in (14). Some of them can be grouped reducing this number to the following variables: K_{11}/γ, $K_{21}-T_{g1}$, K_{12}/γ, $K_{22}-T_{g2}$, $\hat{V}_1^*$, $\hat{V}_2^*$, D_0, E, , ξ, and χ, that must be determined to estimate mutual diffusivities. All of these parameters have physical significance, and therefore one must be able to evaluate every parameter from sources other than diffusion studies. The guidelines to calculate them, clarified by Zielinski and Duda (1992), were used in this work. Additionally the modification proposed by Wang *et al.* (2007), according to the Sanchez-Lacombe equation-of-state (SL EOS), was also taken in account and is explained in Appendix A. The process was considered to be isotermic and isobaric (T=298K, P=1bar and E=0). All the parameters are listed in Table 1 and more details can be found in Appendix A.

Table 1: Model Parameters.

$\hat{V}_1^*$	0.9695 cm^3/mol	(K_{11}/γ)	0.983 x 10^{-3}
$\hat{V}_2^*$	0.8181 cm^3/mol	ρ^*	1.1427 g/cm^3
δ_1	18.29 J$^{1/2}$/cm$^{3/2}$	T^*	668 K
δ_2	20.85 J$^{1/2}$/cm$^{3/2}$	P^*	4035 bar
D_0 x 10^4	14.3 cm^2/s	T_{g2}	213 K
K_{21}-T_{g1}	-12.12		

The numerical values of number- and volume-average (size and standard deviation) – measured with ZetaSizer Nano® from samples all prepared according to the same methodology – are described in Table 2.

4. NUMERICAL SIMULATION

Experimentally the mean diameter is measured by *Dynamic Light Scattering* (ZetaSizer Nano® – Malvern). Typical number and volume density distributions, measured, can be seen in Fig. 2.

According to Table 2 and Fig. 2, it is observed that: (a) The number-average size is always smaller than the volume-average, as the contribution of a spherical particle grows proportionally with D^3; (b) The standard deviation is about 32 – 41% of the averaged value; and, (c) The size distribution does not follow a normal distribution.

Table 2: Number and Volume average sizes.

	Number-average particle diameter	Volume-average particle diameter
Sample 1	222.12 ± 71.25	303.76 ± 103.68
Sample 2	199.23 ± 67.83	285.13 ± 103.97
Sample 3	200.81 ± 73.60	300.90 ± 117.73
Sample 4	200.57 ± 72.48	303.66 ± 126.88

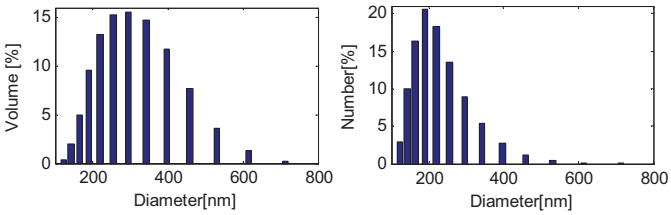

Fig. 2: Measured Number and Volume density distribution.

If it is assumed that the number of droplets/particles remains constant during all the process, the initial distribution can be calculated through the mass balance and based on the experimentally volume density distribution at final time, as explained by Fig. 3.

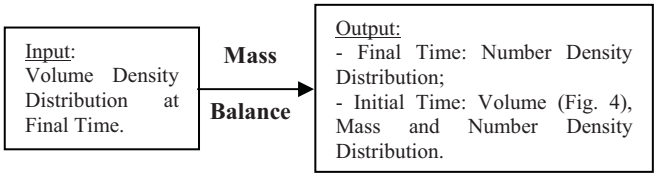

Fig. 3: Measured number and volume size distribution.

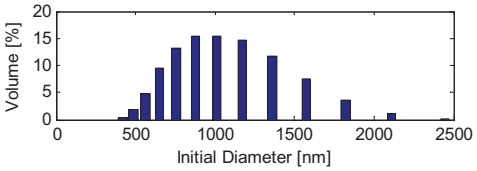

Fig. 4: Calculated Initial Size Distribution.

The calculated number density at final time was compared to the measured one, as can be seen in Fig. 5. The good agreement between both assures that the methodology used in this work is correctly applied.

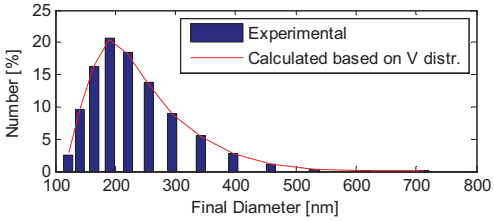

Fig. 5: Comparison between the Experimental and Calculated Number Density Size Distribution.

As the initial size distribution is now available, the diffusion

model can be simulated. It was done in Maple, which is capable of finding solutions for higher order PDE or PDE systems.

Based on the initial size distribution, (5) is solved for each class of particle size. After that, the new radius can be thus calculated. If the relative difference (*ΔDiam*) between the new and old radius is less than $1x10^{-5}$, the process ends; if not, the iteration process goes on as illustrated in Fig. 6.

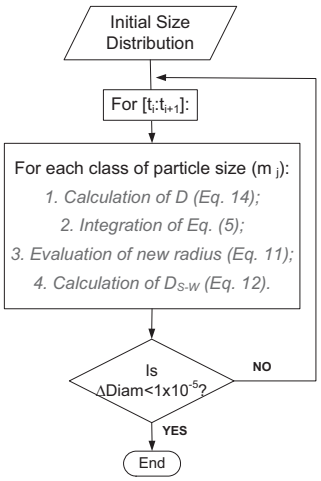

Fig. 6: Scheme of solution implemented in MAPLE.

5. RESULTS AND DISCUSSION

The model predicts that in about 12 ms all the particles reach the final diameter. This result is in qualitative agreement with what is observed experimentally, that is, as the organic phase is mixed in the aqueous phase, the suspension becomes *immediately* (at least for the human eyes) opaque, as a result of the nanoparticle formation.

Throughout the diffusion process, gradients of oil, acetone and polymer arise into the droplet leading to the reduction in size and the formation of the nanoparticle, as can be seen in Fig. 7. Each line represents one class of particle that forms the distribution.

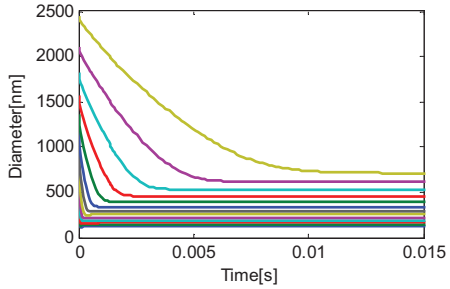

Fig. 7: Evolution of Particle Size in time.

For the smallest particles, it is observed that the diameter reduction is very fast, which is a consequence of the fast diffusion of acetone to the external medium, as can be seen in Fig. 8.

The order of magnitude of the diffusion time is in agreement with that found by Moinard-Chécot *et al.* (2008). They tried to measure the duration of the solvent diffusion step with a stopped-flow apparatus. In this experiment, only the signal corresponding to the final state could be observed, i.e., the diffusion step is less than 20 ms (the acquisition time of the apparatus).

Meanwhile the biggest particles presented a slower diffusion profile. Because of their initial big size, it takes longer for the solvent to reach the interface and consequently, to be transferred to the external medium. As more solvent diffuses out of the droplet, the concentration of polymer inside the droplet increases and consequently, the diffusivity polymer/solvent also grows up. At intermediate steps, the slow reduction in size showed by the largest particles leads almost to a bimodal volume and mass density distribution, as can be seen in Fig. 9.

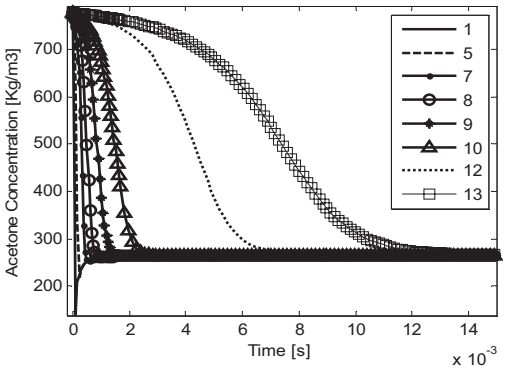

Fig. 8: Acetone concentration at the interface.

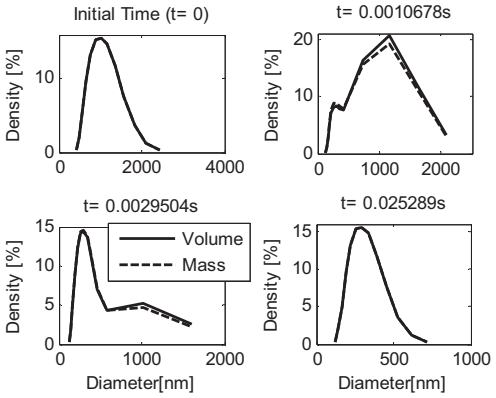

Fig. 9: Volume and Mass Distribution at the initial and final time, and 2 instants of time in-between.

The comparison between the experimental and calculated final volume density distribution (Fig. 10) shows a very good agreement, confirming that the assumptions done in sections 2 and 3 are suitable for modelling the system.

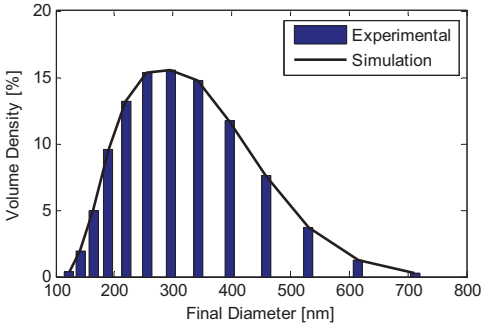

Fig. 10: Comparison between the experimental and simulated volume density distribution.

In order to generalize the model, a probability density

distribution can be employed to describe the initial size of the droplets. Applying the gamma distribution it is possible then to compare the experimental and simulation results, as show in Fig. 11. Analyzing both results and considering the standard deviation of the measurement, it is possible to confirm that the model and the methodology presented in this work are suitable to simulate the nanoprecipitation.

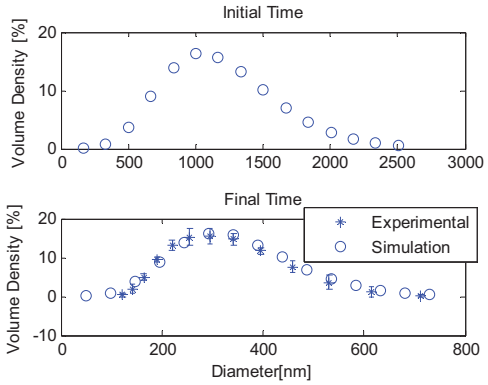

Fig. 11: Results obtained when using a gamma distribution to describe the droplets initial size. (a) Initial size distribution, (b) Final size distribution.

6. CONCLUSIONS

This work shows that it is possible to obtain satisfactory results using a simplified PDE model for the nanoprecipitation. The adopted approach considers several variables that have influence on diffusion, like type of polymer, solvent and non-solvent; affinity among them; and, polymer solubility. As a result, it is then possible to evaluate the particle size distribution during the nanoprecipitation. The comparison between the simulated and measured sizes showed a quite good agreement, suggesting that the employed methodology can describe correctly the nanoprecipitation.

The proposed model can be combined with CFD simulator in order to improve the predictions. From the simulation, one could try to evaluate more accurately the initial droplet distribution. This methodology could thus be applied to study the influence of several kinds and sizes of reactors and mixers in the final properties of the nanoparticles.

Acknowledgments: Prof. Wolfgang Marquardt (PT.AVT – RWTH Aachen) and CNPq/DAAD.

7. REFERENCES

Bearman, R. J. (1961) On the Molecular Basis of some Current Theories of Diffusion. *J. Phys. Chem.,* 65**,** 1961-1968.

Bilati, U., Allemann, E. and Doelker, E. (2005) Development of a nanoprecipitation method intended for the entrapment of hydrophilic drugs into nanoparticles. *European Journal of Pharmaceutical Sciences,* 24**,** 67-75.

Chorny, M., Fishbein, I., Danenberg, H. D. and Golomb, G. (2002) Lipophilic drug loaded nanospheres prepared by nanoprecipitation: effect of formulation variables on size, drug recovery and release kinetics. *Journal of Controlled Release,* 83**,** 389-400.

Crowe, C. T. (2005) *Multiphase Flow Handbook*, CRC Taylor & Francis.

Des Rieux, A., Fievez, V., Garinot, M., Schneider, Y.-J. and Préat, V. (2006) Nanoparticles as potential oral delivery systems of proteins and vaccines: A mechanistic approach. *Journal of Controlled Release,* 116**,** 1-27.

Fessi, H., Puisieux, F., Devissaguet, J. P., Ammoury, N. and Benita, S. (1989) Nanocapsule formation by interfacial polymer deposition following solvent displacement. *International Journal of Pharmaceutics,* 55**,** R1-R4.

Flory, P. J. (1970) Thermodynamics of Polymer Solutions. *Disc. Faraday Soc.,* 49**,** 7 - 29.

Frick, T. S., Huang, W. J., Tirrell, M. and Lodge, T. P. (1990) Probe diffusion in polystyrene/toluene solutions. *Journal of Polymer Science Part B: Polymer Physics,* 28**,** 2629-2649.

Galindo-Rodriguez, S., Allémann, E., Fessi, H. and Doelker, E. (2004) Physicochemical Parameters Associated with Nanoparticle Formation in the Salting-Out, Emulsification-Diffusion, and Nanoprecipitation Methods. *Pharmaceutical Research,* 21**,** 1428-1439.

Galindo-Rodriguez, S. A., Puel, F., Briancon, S., Allemann, E., Doelker, E. and Fessi, H. (2005) Comparative scale-up of three methods for producing ibuprofen-loaded nanoparticles. *European Journal of Pharmaceutical Sciences,* 25**,** 357-367.

Govender, T., Stolnik, S., Garnett, M. C., Illum, L. and Davis, S. S. (1999) PLGA nanoparticles prepared by nanoprecipitation: drug loading and release studies of a water soluble drug. *Journal of Controlled Release,* 57**,** 171-185.

Guterres, S. S., Fessi, H., Barratt, G., Devissaguet, J. P. and Puisieux, F. (1995) Poly (DL-lactide) nanocapsules containing diclofenac: I. Formulation and stability study. *International Journal of Pharmaceutics,* 113**,** 57-63.

Hansen, C. M. (2000) *Hansen solubility parameters: a user's handbook*, CRC Press

Jabr-Milane, L., Van Vlerken, L., Devalapally, H., Shenoy, D., Komareddy, S., Bhavsar, M. and Amiji, M. (2008) Multi-functional nanocarriers for targeted delivery of drugs and genes. *Journal of Controlled Release,* 130**,** 121-128.

Lodge, T. P., Lee, J. A. and Frick, T. S. (1990) Probe diffusion in poly (vinyl acetate) / toluene solutions. *Journal of Polymer Science Part B: Polymer Physics,* 28**,** 2607-2627.

Moinard-Chécot, D., Chevalier, Y., Briançon, S., Beney, L. and Fessi, H. (2008) Mechanism of nanocapsules formation by the emulsion-diffusion process. *Journal of Colloid and Interface Science,* 317**,** 458-468.

Rielly, C. D. and Marquis, A. J. (2001) A particle's eye view of crystallizer fluid mechanics. *Chemical Engineering Science,* 56**,** 2475-2493.

Rodgers, P. A. (1993) Pressure-volume-temperature relationships for polymeric liquids: A review of equations of state and their characteristic parameters for 56 polymers. *Journal of Applied Polymer Science,* 48**,** 1061-1080.

Sugden, S. (1927) Molecular Volumes at Absolute Zero: II. Zero Volumes and Chemical Composition. *Journal of the Chemical Society***,** 1786 - 1798.

Thioune, O., Fessi, H., Devissaguet, J. P. and Puisieux, F. (1997) Preparation of pseudolatex by nanoprecipitation: Influence of the solvent nature on intrinsic viscosity and interaction constant. *International Journal of Pharmaceutics,* 146**,** 233-238.

Van Dijk, M. A. and Wakker, A. (1997) *Polymer Thermodynamics Library - Volume 2: Concepts of Polymer Thermodynamics*.

Van Krevelen, D. W. (1990) *Properties of Polymers*, Elsevier.

Vrentas, J. S. and Duda, J. L. (1976) Diffusion of Small Molecules in Amorphous Polymers. *Macromolecules,* 9**,** 785-790.

Vrentas, J. S. and Duda, J. L. (1977a) Diffusion in Polymer-Solvent Systems. I. Reexamination of the Free-Volume Theory. *J. Polymer Sci., Polymer Phys.,* 15**,** 403 - 416.

Vrentas, J. S. and Duda, J. L. (1977b) Diffusion in Polymer-Solvent Systems. II. A Predictive Theory for the Dependence of Diffusion Coefficients on Temperature, Concentration, and Molecular Weight. *J. Polymer Sci., Polymer Phys.,* 15**,** 417 - 439.

Vrentas, J. S. and Duda, J. L. (1979) Molecular Diffusion in Polymer Solutions. *AIChE J.,* 25**,** 1 - 24.

Wang, B.-G., Lv, H.-L. and Yang, J.-C. (2007) Estimation of solvent diffusion coefficient in amorphous polymers using the Sanchez-Lacombe equation-of-state. *Chemical Engineering Science,* 62**,** 775-782.

Wild, A. (2003) Multicomponent Diffusion in Liquids. TU München.

Zielinski, J. M. and Duda, J. L. (1992) Predicting polymer/solvent diffusion coefficients using free-volume theory. *AIChE Journal,* 38**,** 405-415.

Appendix A. FREE VOLUME THEORY PARAMETERS

$\hat{V}_1^*$ *and* $\hat{V}_2^*$ – The two critical volumes were approximated as the specific volumes of solvent and polymer at absolute zero temperature. The molar volumes at 0K were estimated using a group contribution method (Sugden, 1927).

χ – The interaction parameter in terms of solubility parameters can be calculated through the following equation (Van Dijk and Wakker, 1997):

$$\chi = \frac{V_m}{RT}(\delta_1 - \delta_2)^2 \tag{15}$$

where V_m is the molar volume, R is the ideal gas constant and δ_1 and δ_2 are the solvent and polymer solubility parameters respectively.

A widely used solubility parameter approach for predicting polymer solubility is proposed by Hansen (2000). The basis of the so-called Hansen Solubility Parameters (HSP) is that the total energy of vaporization of a liquid consists of several individual parts. These arise from (atomic) dispersion forces (E_D), (molecular) permanent dipole-permanent dipole forces (E_P) and (molecular) hydrogen bonding (electron exchange) (E_H). The basic equation which governs the assignment of Hansen parameters is that the total cohesion energy, E, must be the sum of the individual energies which make it up

$$E = E_D + E_P + E_H \tag{16}$$

Dividing each one by the molar volume gives the square of the total solubility parameter.

$$\begin{aligned} E/V &= E_D/V + E_P/V + E_H/V \\ \delta^2 &= \delta_D^2 + \delta_P^2 + \delta_H^2 \end{aligned} \tag{17}$$

The solubility parameter components were predicted from group contribution method, using the following equations (Van Krevelen, 1990).

$$\delta_d = \sum F_{di} \Big/ V \qquad \delta_p = \sqrt{\sum F_{pi}^2} \Big/ V \qquad \delta_h = \sqrt{\sum E_{hi} \Big/ V} \tag{18}$$

D_0, K_{21}-T_{g1}, (K_{11}/γ) – These are solvent parameters (acetone) and the values previously collected by Zielinski and Duda (1992) were used here.

$(K_{12}/\gamma)(K_{22}$-T_{g2}+$T)$(Wang et al., 2007) – According to the Vrentas-Duda model (Zielinski and Duda, 1992), the hole free volume of a polymer $\hat{V}_{FH2}$ in its rubbery state can be expressed as

$$\frac{\hat{V}_{FH2}}{\gamma} = (K_{12}/\gamma)(K_{22} - T_{g2} + T) \tag{19}$$

Assuming that the hole free volume is equal to the volume defined by the WLF (Williams, Landel and Ferry) theory, at the atmospheric pressure, (19) becomes

$$\frac{\hat{V}_{FH2}}{\gamma} = V\left\{0.025 + \int_{T_{g2}}^{T}\left[\left(1+\frac{\tilde{P}}{\tilde{\rho}^2}\right)\Big/\left(T\left[\frac{\tilde{T}}{1-\tilde{\rho}} - 2\right]\right)\right]_{P0} dT\right\} \tag{20}$$

where $V(=1/\rho)$ is the volume of polymer per gram at temperature T, which can be estimated by the SL EOS according to the equation,

$$\tilde{\rho} = 1 - \exp\left[-\left(\tilde{\rho}^2 + \tilde{P}\right)/\tilde{T} - \tilde{\rho}\right] \tag{21}$$

with the definition

$$\tilde{\rho} = \rho/\rho^*, \qquad \tilde{T} = T/T^*, \qquad \tilde{P} = P/P^* \tag{22}$$

where ρ^*, T^* and P^* are characteristics parameters of mass density, temperature and pressure, respectively. These parameters are listed by Rodgers (1993) and those for PCL used in this work are listed in Table 1. This method eliminates the need to use polymer viscoelastic data for determining the polymer free volume parameters. Additionally, its scope is also extended to include not only temperature and concentration but also pressure influence on solvent diffusivities. The only new parameters introduced by this model (ρ^*, T^* and P^*) are three parameters of the SL EOS (Wang et al., 2007).